

Ant-Colony-Based Multiuser Detection for Multi-Functional Antenna Array Assisted MC DS-CDMA Systems

C. Xu, B. Hu, L.-L. Yang, *Senior Member, IEEE*, and L. Hanzo, *Fellow, IEEE*

Abstract—A novel Ant Colony Optimization (ACO) based Multi-User Detector (MUD) is designed for the synchronous Multi-Functional Antenna Array (MFAA) assisted Multi-Carrier Direct-Sequence Code-Division Multiple-Access (MC DS-CDMA) uplink (UL), which supports both receiver diversity and receiver beamforming. The ACO-based MUD aims for achieving a bit-error-rate (BER) performance approaching that of the optimum maximum likelihood (ML) MUD, without carrying out an exhaustive search of the entire MC DS-CDMA search space constituted by all possible combinations of the received multi-user vectors. We will demonstrate that regardless of the number of the subcarriers or of the MFAA configuration, the system employing the proposed ACO based MUD is capable of supporting 32 users with the aid of 31-chip Gold codes used as the T-domain spreading sequence without any significant performance degradation compared to the single-user system. As a further benefit, the number of floating point operations per second (FLOPS) imposed by the proposed ACO-based MUD is a factor of 10^8 lower than that of the ML MUD. We will also show that at a given increase of the complexity, the MFAA will allow the ACO based MUD to achieve a higher SNR gain than the Single-Input Single-Output (SISO) MC DS-CDMA system.

Index Terms—Ant Colony Optimization, Multi-User Detector, Multi-Functional Antenna Array, Multi-Carrier Direct-Sequence Code-Division Multiple-Access, Uplink, Near-Maximum Likelihood Detection.

I. INTRODUCTION

Multi-Carrier Direct Sequence Code Division Multiple Access (MC DS-CDMA) is widely recognized as a high-flexibility multiple-access scheme [1]–[6], which is based on a combination of DS-CDMA and OFDM. In this treatise, we further develop the generalized MC DS-CDMA system investigated in [7], [8], which includes the subclasses of both multitone DS-CDMA [2] and orthogonal MC DS-CDMA [3] as special cases. **Explicitly, our first contribution is that we proposed an amalgamated uplink receiver diversity and receiver beamforming aided MC DS-CDMA scheme for improving the achievable performance of generalized MC DS-CDMA systems.** These diversity-aided beamformers are capable of selectively receiving energy from the intended directions of the desired users, which potentially reduces

the interference amongst wireless users [9], [10], as well as mitigating the effects of fading.

Unlike in [11]–[13], where orthogonal Walsh Hadamard codes were employed as the T-domain spreading sequences, in this paper, non-orthogonal codes are employed, resulting in multi-user interference (MUI), which requires the employment of multi-user detection (MUD) [4], [14]. The optimal maximum likelihood (ML) MUD carries out an exhaustive search for all the legitimate combinations of the transmit symbols of all the users. Naturally, this technique has a complexity that increases exponentially with the number of users, as well as with the number of bits per symbol, which motivates the development of reduced-complexity near-optimum MUDs. For instance, genetic algorithms (GA) [4], [15], [16], evolutionary programming [17], particle swarm optimization [18], ant-colony optimization (ACO) [19]–[21], sphere decoding [22], [23] and Markov-Chain Monte-Carlo (MCMC) [24] aided detectors have found favour in low-complexity near-optimum MUDs.

As our second contribution, we develop a sophisticated near-ML and yet low-complexity ACO based MUD designed for the proposed novel multi-functional antenna array (MFAA) assisted synchronous MC DS-CDMA uplink (UL). The ACO technique has been shown to outperform GAs in some NP-complete optimization problems, such as the travelling salesman problem [20]. Moreover, according to [25]–[28], the ACO based MUDs are capable of achieving a lower BER and a lower complexity than the GA-based MUDs.

The rest of this paper is organized as follows. The MFAA assisted MC DS-CDMA system model will be described in Section II. In Section III, the ACO algorithm as well as its MFAA assisted MC DS-CDMA version will be detailed. Both the achievable BER performance and the complexity imposed will be quantified in Section IV. Finally, we will conclude our discourse in Section V.

II. SYSTEM DESCRIPTION

In this section, the generalized MC DS-CDMA system of Fig. 1 [7], [8], [29] is reviewed. At the transmitter side, the binary data stream having a bit duration of T_b is Serial-to-Parallel (S/P) converted to U parallel sub-streams. The new bit duration of each sub-stream, which we refer to as the symbol duration, becomes $T_s = UT_b$. After S/P conversion, each substream is spread using an N_c -chip DS spreading sequence waveform $c_k(t)$. Then, the DS-spread signal of the

Acknowledgements: The financial support of the EPSRC, UK and that of the EU under the auspices of the PHOENIX and NEWCOM projects and the Dorothy Hodgkin Postgraduate Awards is gratefully acknowledged.

C. Xu, L.-L. Yang and L. Hanzo are with School of ECS, University of Southampton, Southampton, UK. E-mail: {cx05r, lly, lh}@ecs.soton.ac.uk.

B. Hu was with School of ECS, University of Southampton, Southampton, UK. He is now with Samsung Electronics Research Institute, Staines TW18 4QE, UK. E-mail: b.hu@samsung.com.

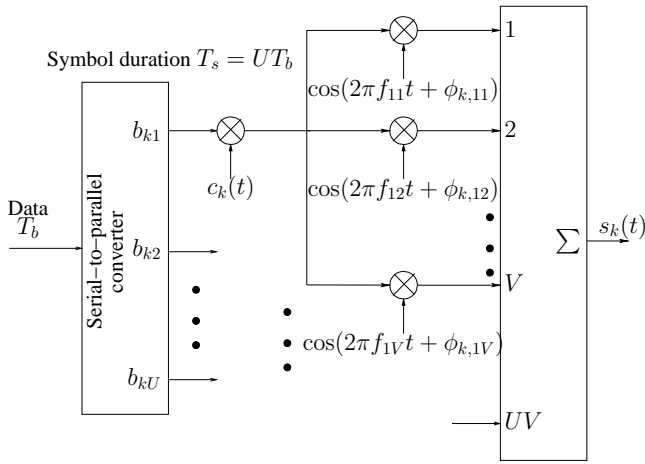


Fig. 1. The k th user's UL transmitter schematic for the generalized multicarrier DS-CDMA system.

u th sub-stream, where we have $u = 1, 2, \dots, U$, simultaneously modulates a group of parallel subcarrier frequencies $\{f_{u1}, f_{u2}, \dots, f_{uV}\}$ using Binary Phase Shift Keying (BPSK). Thus the signal transmitted on the uv th subcarrier of user k can be expressed as $s_{k,uv}(t) = \sqrt{2P/V} b_{ku}(t) c_k(t) \cos(2\pi f_{uv}t + \phi_{k,uv})$, where P/V represents the transmitted power of each subcarrier and P is the transmitted power corresponding to each bit. Furthermore, $\{b_{ku}(t)\}$, $\{f_{uv}\}$ and $\{\phi_{k,uv}\}$ represent the subcarrier data streams, the subcarrier frequency set and the phase angles introduced in the carrier modulation process. A total of UV number of subcarriers are required in the MC DS-CDMA system considered and the UV number of subcarrier signals are superimposed on each other in order to form the complex modulated signal. Therefore, the transmitted signal of user k can be expressed as $s_k(t) = \sum_{u=1}^U \sum_{v=1}^V \sqrt{2P/V} b_{ku}(t) c_k(t) \cos(2\pi f_{uv}t + \phi_{k,uv})$.

We assume that at the base-station (BS) there are N_r number of receiver antenna arrays, as shown in Fig.2, which are located sufficiently far apart so that the corresponding received MC DS-CDMA signals experience independent fading when they reach the different antenna arrays. Each of the N_r antenna arrays consists of L number of elements separated by a distance of d , which is usually half a wavelength. Hence the system benefits from both receiver diversity and receiver beamforming. For simplicity, we assume that there is no angular spread. Then the Spatio-Temporal Channel Impulse Response (ST-CIR) $h_{uv}^{(nr,l)}$ between the uv th subcarrier of the k th user and the l th array element of the n_r th antenna can be expressed as $h_{uv,k}^{(nr,l)} = h_{uv,k}^{(nr,0)}(t) \exp\{j \cdot 2\pi d/\lambda \cdot l \cdot \sin[\psi_k^{(nr)}]\} \delta(t - \tau_k)$, $n_r = 0, 1, \dots, N_r - 1$; $l = 0, 1, \dots, L - 1$; $u = 1, 2, \dots, U$; $v = 1, 2, \dots, V$; $k = 1, 2, \dots, K$, where τ_k is the signal's delay, $h_{uv,k}^{(nr,0)}(t)$ is the Rayleigh faded envelope from the k th user to the 1st element of the n_r th antenna array, λ is the wavelength and $\psi_k^{(nr)}$ is the average Direction-Of-Arrival (DOA) from the k th user to the n_r th antenna array. In this paper, the distribution of the users' DOAs at the base station is determined using the Geometrically Based Single Bounce Circular Model (GBSBCM) [30], where the

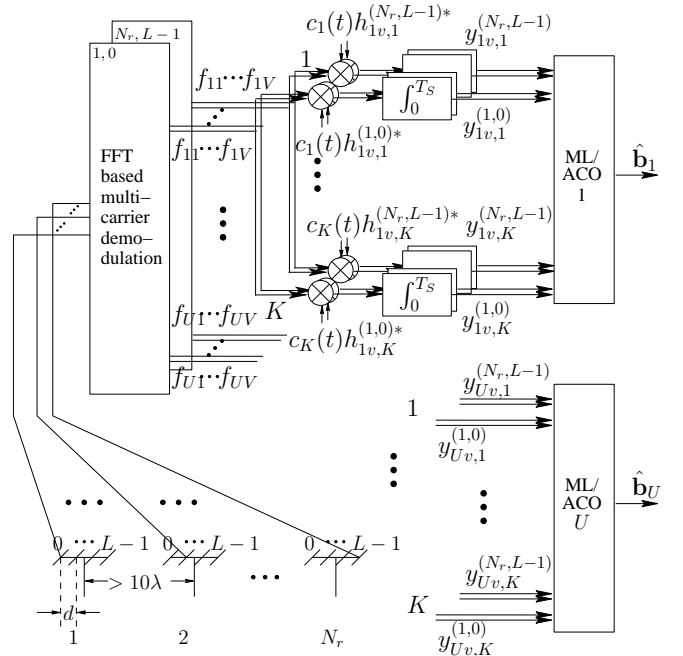


Fig. 2. Uplink receiver block diagram of the generalized MC DS-CDMA system considered for all the K users when employing the maximum likelihood detector or the ACO-based MUD. Note that every symbol v in the figure represents all the $v = 1, \dots, V$.

average DOA is the DOA of the line-of-sight (LOS) path. Slow DOA evolution was assumed for each user and hence the users' DOAs may judiciously be assumed to remain fixed during each received burst.

We assume that K synchronous MC DS-CDMA users are supported by the system. Furthermore, we assume that the subcarrier signals are orthogonal to each other. Hence, we can consider the received signal on a subcarrier by subcarrier basis. Thus the $(N_c \times 1)$ -dimensional received signal vector containing the signals of all the K users associated with the uv th subcarrier at the n_r th antenna's l th element can be expressed as $\mathbf{r}_{uv}^{(nr,l)} = \mathbf{C} \mathbf{H}_{uv}^{(nr,l)} \xi \mathbf{b}_u + \mathbf{n}_{uv}^{(nr,l)}$, where $\xi = \sqrt{P/V}$ and \mathbf{C} represents the $(N_c \times K)$ -dimensional spreading code matrix. Furthermore, $\mathbf{H}_{uv}^{(nr,l)}$ is a $(K \times K)$ -dimensional matrix, where the diagonal elements of $\mathbf{H}_{uv}^{(nr,l)}$ represent the ST-CIRs of all the users modulating the uv th subcarrier and impinging at the l th element of the n_r th MFAA, which is formulated as $\mathbf{H}_{uv}^{(nr,l)} = \text{diag}[h_{uv,1}^{(nr,l)}, h_{uv,2}^{(nr,l)}, \dots, h_{uv,K}^{(nr,l)}]$. Finally, \mathbf{b}_u represents the $(K \times 1)$ -dimensional vector of signals to be transmitted by all the K users associated with the u th branch and $\mathbf{n}_{uv}^{(nr,l)}$ is the $(N_c \times 1)$ -dimensional additive white Gaussian noise (AWGN) vector, where each element has a zero mean and a variance of $2N_0$.

For simplicity, we assume that the ST-CIRs are perfectly known at the BS. It can be shown that the $(K \times 1)$ -dimensional MRC based MF's output vector corresponding to the uv th subcarrier of all the K users at the l th element of the n_r th MFAA can be expressed as $\mathbf{y}_{uv}^{(nr,l)} = (\mathbf{C} \mathbf{H}_{uv}^{(nr,l)})^H \mathbf{r}_{uv}^{(nr,l)} = \mathbf{H}_{uv}^{(nr,l)H} \mathbf{C}^T \mathbf{C} \mathbf{H}_{uv}^{(nr,l)} \xi \mathbf{b}_u + \mathbf{H}_{uv}^{(nr,l)H} \mathbf{C}^T \mathbf{n}_{uv}^{(nr,l)} = \mathbf{R}_{uv}^{(nr,l)} \xi \mathbf{b}_u +$

$\tilde{\mathbf{n}}_{uv}^{(n_r,l)}$, where we have

$$\mathbf{R}_{uv}^{(n_r,l)} = \mathbf{H}_{uv}^{(n_r,l)H} \mathbf{C}^T \mathbf{C} \mathbf{H}_{uv}^{(n_r,l)}, \quad (1)$$

and each element in $\tilde{\mathbf{n}}_{uv}^{(n_r,l)}$ has a mean of zero and a variance of $2N_0$. By adding up the matched filter outputs of all the V subcarriers, the L elements and the N_r antenna arrays, the superposition of the matched filter outputs can be formulated as $\mathbf{z}_u = \sum_{n_r=1}^{N_r} \sum_{l=0}^{L-1} \sum_{v=1}^V y_{uv}^{(n_r,l)} = L \left[\sum_{n_r=1}^{N_r} \sum_{v=1}^V \|\mathbf{H}_{uv}^{(n_r,0)}\|^2 \right] \xi \mathbf{b}_u + L\xi \mathbf{I}_u + \sum_{n_r=1}^{N_r} \sum_{l=0}^{L-1} \sum_{v=1}^V \tilde{\mathbf{n}}_{uv}^{(n_r,l)}$. If the MUI component \mathbf{I}_u of the u th branch can be eliminated by the receiver, the average SNR at the input of the MFAA-assisted MC DS-CDMA system's BPSK demodulator can be formulated as

$$\bar{\Upsilon}_S^{\text{MFAA}} = \frac{\mathcal{E}\{\text{signal}^2\}}{\mathcal{E}\{\text{noise}^2\}} = \frac{PL^2 N_r^2 V^2 / V}{N_r V L \sigma_n^2} = LN_r \bar{\Upsilon}_S^{\text{SISO}}, \quad (2)$$

which is LN_r times higher than the average SNR in its SISO counterpart $\bar{\Upsilon}_S^{\text{SISO}}$.

III. ANT COLONY OPTIMIZATION BASED MULTIUSER DETECTOR

The ACO algorithm [25]–[28] is based on the foraging behavior of the ant colony in nature. Every ant leaves pheromone along the route from the formic nest to a certain remote source of food. Therefore, the shorter the route, the more the pheromone. As a beneficial effect of the pheromone, the ants about to set out from the nest later are more likely to choose the particular route marked by a higher concentration of pheromone. As a result, most ants will choose the shortest route from the nest to the source of food.

As seen in Fig. 2, each of the U substream's ACO-based MUDs generates a $(K \times 1)$ -dimensional vector, say $\hat{\mathbf{b}}_u$, for the K -user transmit signal vector of the u th substream bit, say \mathbf{b}_u . Remembering that the different subcarrier signals are orthogonal, the U number of ACO-based MUDs may operate in parallel without interfering with each other. Hence, we omit the index u for notational convenience in the following review of the ACO algorithm throughout Subsection III-A. We assume furthermore that a maximum of N iterations are affordable in complexity terms, when searching for the best route in each ACO-based MUD. The flow chart of the ACO-based MUD algorithm is depicted in Fig. 3.

A. Review of the Algorithm

	1	2	...	K
1	$b_1 = +1$	$b_2 = +1$...	$b_K = +1$
2	$b_1 = -1$	$b_2 = -1$...	$b_K = -1$

Route-Matrix and Generation of Vectors In every ACO-aided MUD, there is a so-called route-matrix or route-table comprising K columns and two rows. The K columns represent the K number of users and the two rows correspond to the two legitimate values of $+1$ and -1 of the BPSK signal of each user. By opting for one of the two legitimate values of each column, we arrive at a K -element vector, which constitutes a

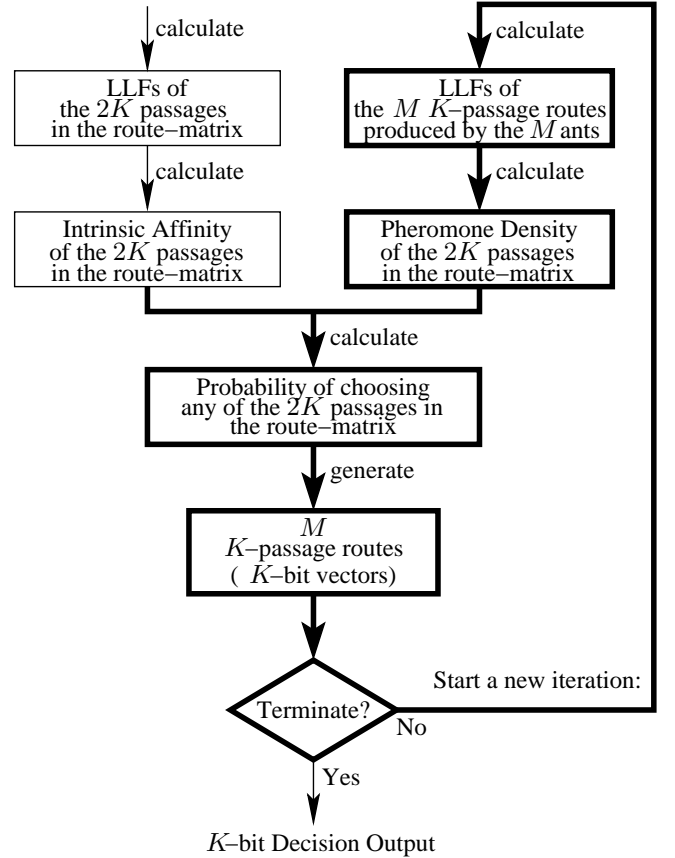


Fig. 3. Flow chart of the ACO MUD. All the processes marked by bold lines are repeatedly carried out in every iteration and all the values in the bold rectangles will be changed in each iteration.

candidate to be chosen as the final decision output of the ACO-aided MUD. From an ant's perspective, each vector represents a unique route consisting of K passages from the left of the route-table to the right. Hence the route-matrix or route-table comprises a total of $2K$ passages and each passage can be uniquely represented by a specific transmitted bit. For instance, the passage associated with the 1st row of the 2nd column can be expressed as $\{b_2 = +1\}$. Later we will show that every single passage in the route-table is associated with an *intrinsic* affinity value, which represents the probability of the ant colony choosing that particular passage before any ant has crossed the passage. Similarly, the *extrinsic* pheromone value is associated with the same passage after the 1st iteration and quantifies the merit of that passage after the entire ant colony have tamped across that passage. These two values jointly determine the ant colony's future preferences concerning a certain passage from the 2nd iteration on.

Intrinsic Affinity The intrinsic affinity value of the two passages represented by $\{b_k = \pm 1\}$ are determined by their Log Likelihood Functions (LLFs), which are deduced from the natural logarithm of the *a priori* probability $p\{y_k | b_k = \pm 1\}$ [31], given that y_k is the matched filter output of the k th user and b_k is the transmitted signal. More quantitatively, let us first of all introduce the so-called desirability function of $\{b_k = \pm 1\}$, which can be expressed as $\gamma_{k,\pm 1} = 1 + \exp[-ll f_k(\pm 1)]$,

for $k = 1, \dots, K$ [28], where $llf_k(\pm 1)$ represent the LLFs of $\{b_k = \pm 1\}$. Given the desirability function, the intrinsic affinity values of $\{b_k = \pm 1\}$ may be expressed as $\omega_{k,\pm 1} = \eta_{k,\pm 1}^\beta = [\sum_{i \in \{+1, -1\}} \gamma_{k,i} / \gamma_{k,\pm 1}]^\beta$, $k = 1, \dots, K$ [28], where β is a tunable weighting or de-weighting parameter.

Pheromone The pheromone is updated during every iteration after the M routes (vectors) have been generated. We use a $(2 \times K)$ -dimensional matrix to represent the pheromone values corresponding to the $2K$ passages in the route-table. The pheromone values deposited along the $2K$ passages during the first iteration are initialized as $\tau_{k,\pm 1}^{(1)} = 0.01$, $k = 1, \dots, K$ [28]. In order to update the pheromone, two different types of *incremental* pheromone matrices will be added to the existing pheromone matrix.

One of them is the so-called *mass* incremental pheromone matrix. As implied by the terminology, every ant in every iteration will generate a *mass* incremental pheromone matrix. The positions of the K non-zero elements in $\Delta\tau_m^{(n)}$, which represents the *mass* incremental pheromone matrix generated by the m th ant during the n th iteration, overlap with the particular positions of the K passages in the route-matrix constituting the specific route taken by the ant. More quantitatively, the value of all the K non-zero elements in $\Delta\tau_m^{(n)}$ is given by the LLF value $LLF[\underline{\mathbf{b}}_m^{(n)}]$ of the vector $\underline{\mathbf{b}}_m^{(n)}$ produced by the m th ant. Explicitly, we have $\Delta\tau_m^{(n)} = LLF[\underline{\mathbf{b}}_m^{(n)}] \cdot \underline{\mathbf{B}}_m^{(n)}$ [28], where $\underline{\mathbf{B}}_m^{(n)}$ is the $(2 \times K)$ -dimensional matrix representation of $\underline{\mathbf{b}}_m^{(n)}$. For instance, if we have $\underline{\mathbf{b}}_m^{(n)} = [+1, +1, -1]^T$, we arrive at $\underline{\mathbf{B}}_m^{(n)} = [1 \ 1 \ 0; 0 \ 0 \ 1]$ and $\Delta\tau_m^{(n)} = [LLF[\underline{\mathbf{b}}_m^{(n)}], LLF[\underline{\mathbf{b}}_m^{(n)}], 0; 0, 0, LLF[\underline{\mathbf{b}}_m^{(n)}]]$.

By the contrast, the other type of the above-mentioned incremental pheromone matrix, which is referred to as the *elite* incremental pheromone matrix, may have been produced by a single *elite* ant, i.e. the specific ant that produced the optimal vector. The vector is not necessarily produced during the n th iteration, but it has the highest LLF among all the $n \cdot M$ vectors produced during the previous n iterations. Similar to the *mass* incremental pheromone matrix, all the K non-zero elements in the *elite* incremental pheromone matrix overlap with the particular positions in the route-table constituting the optimal route, which are quantified in terms of the LLF value $LLF[\underline{\mathbf{b}}_*^{(n)}]$ of the optimal vector $\underline{\mathbf{b}}_*^{(n)}$. More explicitly, the *elite* incremental pheromone matrix can be expressed as $\tau_*^{(n)} = \sigma \cdot LLF[\underline{\mathbf{b}}_*^{(n)}] \cdot \underline{\mathbf{B}}_*^{(n)}$, where $\underline{\mathbf{B}}_*^{(n)}$ is the matrix counterpart of $\underline{\mathbf{b}}_*^{(n)}$ and σ is the weighting factor.

While new pheromone is being deposited in the pheromone matrix, the contents of the outdated pheromone matrix $\tau^{(n)}$ will evaporate at the same time. More quantitatively, if we assume that the pheromone evaporates at a rate of ρ , which is an experimentally tuned parameter spanning the range of $(0, 1]$, the pheromone that is finally left for the next iteration is given by $\rho \cdot \tau^{(n)}$. Overall, the updated pheromone matrix $\tau^{(n+1)}$ available for the $(n+1)$ st iteration can be formulated as $\tau^{(n+1)} = \rho \cdot \tau^{(n)} + \sum_{m=1}^M \Delta\tau_m^{(n)} + \tau_*^{(n)}$.

Probability of Choosing a Passage Quantitatively, during the n th iteration, the probability of choosing the passage represented by $\{b_k = +1\}$ in the route-table can be formulated as $p^{(n)}\{b_k = +1\} = \mu_{k,+1}^{(n)} \omega_{k,+1} / \sum_{i \in \{+1, -1\}} \mu_{k,i}^{(n)} \omega_{k,i}$ [28],

where $\mu_{k,\pm 1}^{(n)} = [\tau_{k,\pm 1}^{(n)}]^\alpha$ represent the effect of the pheromone intensities associated with the passages corresponding to $\{b_k = \pm 1\}$ during the n th iteration, where α is a tunable weighting coefficient, while $\omega_{k,\pm 1}$ is constant throughout the N iterations and denotes the intrinsic affinities of the passages represented by $\{b_k = \pm 1\}$. More explicitly, \bar{M} number of ants will follow the passage represented by $\{b_k = +1\}$ during the n th iteration, given that the integer value $\bar{M} = \Gamma[M \cdot p^{(n)}\{b_k = +1\}]$ represents the rounded version of $M \cdot p^{(n)}\{b_k = +1\}$. Naturally, the remaining $(M - \bar{M})$ number of ants will opt for the passage represented by $\{b_k = -1\}$.

Iterative Procedure and its Termination Condition The flow chart of the entire iterative optimization procedure is shown in Fig. 3. The result of the optimization guided by the updating of the pheromone matrix is that the ants are more likely to opt for that particular passage during the *next* iteration, which is part of the optimal vector found so far. Consequently, the probability of the optimal ML vector's appearance during the *next* iteration is increased. The optimization procedure of the ACO-based MUD will terminate at the N_e th iteration, if either all the ants produce the same K -user vector estimate during the N_e th cycle, or all the N number of affordable ACO iterations have been carried out, i.e. we have $N_e = N$. Then, the MUD's output $\hat{\mathbf{b}}$ is given by the optimal vector found so far, i.e. $\hat{\mathbf{b}} = \underline{\mathbf{b}}_*^{(N_e)}$.

B. ACO MUD in the Multi-Functional Antenna Array Assisted MC DS-CDMA Uplink

Firstly, the LLF of a bit $b_{ku} = \dot{b} \in \{\pm 1\}$ transmitted in the u th sub-stream associated with the v th subcarrier and received at the l th element of the n_r th antenna array can be expressed as [31]

$$q_{uv,k}^{(n_r l)}[\dot{b}] = 2\Re\{\xi \dot{b} \cdot y_{uv,k}^{(n_r l)}\} - \xi^2 R_{uv,kk}^{(n_r l)}, \quad \dot{b} \in \{+1, -1\}, \quad (3)$$

where $y_{uv,k}^{(n_r l)}$ is the MF output of the k th user's signal transmitted on the u th sub-stream associated with the v th subcarrier and received at the l th element of the n_r th antenna array and $R_{uv,kk}^{(n_r l)}$ represents the k th diagonal element of $\mathbf{R}_{uv}^{(n_r l)}$ in (1). Furthermore, the LLF of a bit-vector $\mathbf{b}_u = \dot{\mathbf{b}} \in \mathcal{B}_K$ transmitted in the u th sub-stream associated with the v th subcarrier and received at the l th element of the n_r th antenna array can be expressed as [31]

$$Q_{uv}^{(n_r l)}[\dot{\mathbf{b}}] = 2\Re\{\xi \dot{\mathbf{b}}^T \mathbf{y}_{uv}^{(n_r l)}\} - \xi^2 \dot{\mathbf{b}}^T \mathbf{R}_{uv}^{(n_r l)} \dot{\mathbf{b}}, \quad \dot{\mathbf{b}} \in \mathcal{B}_K, \quad (4)$$

where \mathcal{B}_K is the set containing all the 2^K legitimate vectors for K BPSK-modulated bit-combinations.

The LLF values of either a bit being a legitimate value or a vector being a legitimate vector in an MFAA-assisted MC DS-CDMA system are given by the superposition of the LLFs associated with each of the V subcarriers on each of the L antenna element per MFAA and each of the N_r receive

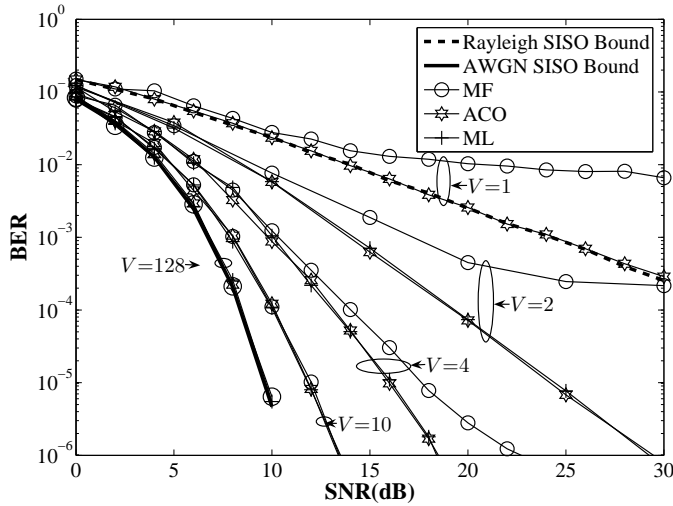


Fig. 4. BER versus SNR performance of the ACO based MUD in the SISO MC DS-CDMA UL, over uncorrelated Rayleigh channels when $N_c = 31$ -chip Gold sequences as employed and $K = 32$ users are supported.

antenna arrays, yielding:

$$llf_{ku}[\dot{\mathbf{b}}] = \zeta \cdot \sum_{n_r=1}^{N_r} \sum_{l=0}^{L-1} \sum_{v=1}^V q_{uv}^{(n_r, l)}[\dot{\mathbf{b}}], \quad \dot{\mathbf{b}} \in \{+1, -1\}; \quad (5)$$

$$LLF_u[\dot{\mathbf{b}}] = \zeta \cdot \sum_{n_r=1}^{N_r} \sum_{l=0}^{L-1} \sum_{v=1}^V Q_{uv}^{(n_r, l)}[\dot{\mathbf{b}}], \quad \dot{\mathbf{b}} \in \mathcal{B}_K. \quad (6)$$

A normalization factor of ζ is introduced in (5) and (6) because the power of the superimposed MF outputs has been enlarged by a factor of $(N_r \cdot L)^2$ as a benefit of using the MFAA configuration, which has been explicitly observed in Eq. (2). Thus the accumulated LLF values in (5) and (6) should be normalized using the weighting coefficient of $\zeta = 1/\sqrt{(N_r \cdot L)^2} = 1/(N_r \cdot L)$, before it is used in the subsequent calculation of the *intrinsic affinity* and *pheromone values* of a certain passage.

IV. SIMULATION RESULTS

Throughout our simulations, we assume that the T-domain spreading sequences were the $N_c = 31$ -chip Gold codes and the parameters of the ACO MUD were set to $\rho = 0.5$, $M = 10$, $N = 10$, $\alpha = 1$, $\beta = 6$ and $\sigma = 8$. The BER performance of the ACO-based MUD, the MRC based MF and the ML MUD of the SISO MC DS-CDMA system are presented in Fig. 4, while the BER performance of the ACO-based MUD employed in the MFAA-assisted MC DS-CDMA system can be observed in Fig. 5. Additionally, the diversity gain $\Delta\Upsilon_D$, array gain $\Delta\Upsilon_A$ as well as the SNR gain $\Delta\Upsilon_S$ versus the number of receive antennas employed in the MFAA-assisted MC DS-CDMA UL is studied in Fig. 6.

Firtstly, as seen in Fig. 4, Fig. 5 and Fig. 7, the ACO-based MUD is capable of approaching the BER performance of the ML MUD at a similarly low complexity as that of the MRC-MF, regardless of the value of V , L or N_r . For instance, when the number of users is $K = 32$, the complexity of the ACO-based MUD may be deemed to be a factor of 10^8 lower than that of the MLD.

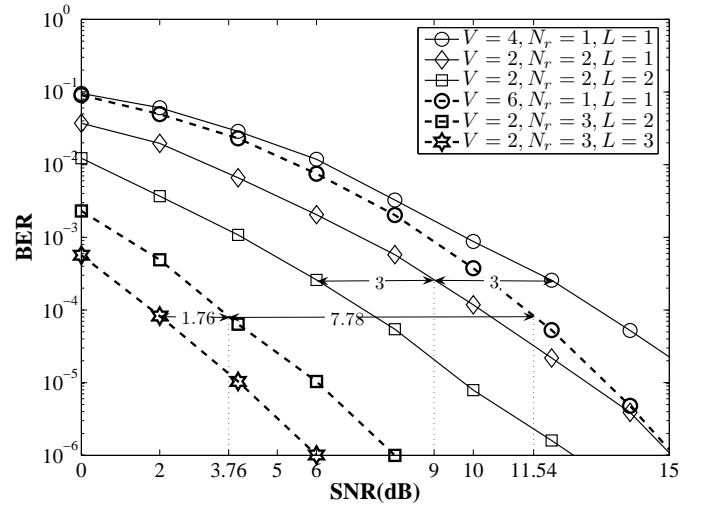


Fig. 5. BER versus SNR performance of the ACO based MUD in the MFAA assisted MC DS-CDMA UL, over uncorrelated Rayleigh channels when $N_c = 31$ -chip Gold sequences are employed and $K = 32$ users are supported.

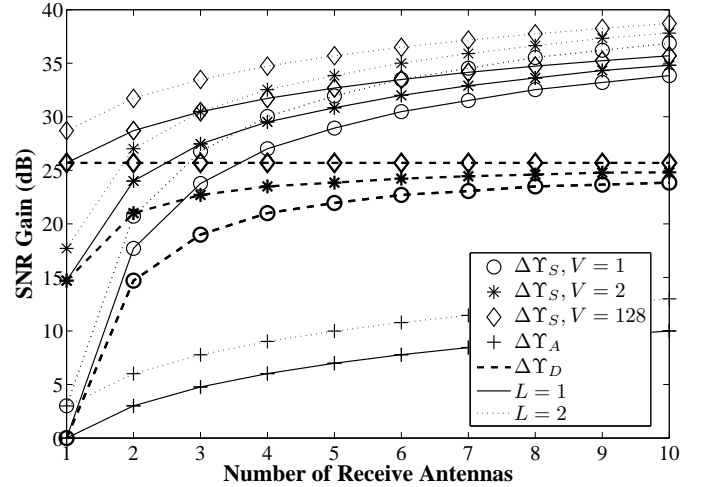


Fig. 6. The diversity gain $\Delta\Upsilon_D$, the array gain $\Delta\Upsilon_A$ and the SNR gain $\Delta\Upsilon_S$ versus the number of receive antennas in conjunction with different number of subcarriers V and with $L = 1$ or 2 elements per antenna array at a BER of 10^{-4} . Uncorrelated Rayleigh channels are considered, $N_c = 31$ -chip Gold sequences are employed and $K = 32$ users are supported.

Secondly, the SNR gain of the MFAA-assisted MC DS-CDMA UL experienced at a certain BER value is the sum of the diversity gain and the array gain. More explicitly, the diversity gain Υ_D is monotonically increasing with the diversity order of $\gamma_d = V \times N_r$, while the array gain Υ_A is directly quantified as $10\lg(\gamma_a) = 10\lg(N_r \times L)$. The array gain $\Delta\Upsilon_A$ experienced at the BER of 10^{-4} attained by the different MFAA-assisted MC DS-CDMA systems having the same diversity gain as the single user SISO DS-CDMA benchmark system has been recorded in Fig. 5.

Thirdly, as seen in Fig. 7, the complexity of the ACO based MUD associated with a low number of subcarriers, such as $V = 2$, but using the $L = 2$ and $N_r = 2$ MFAA-assisted MC DS-CDMA configuration is not as high as that in the SISO MC

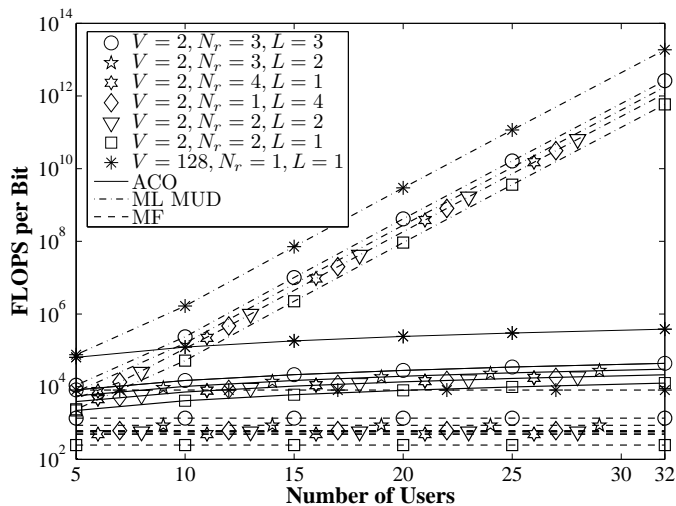


Fig. 7. Complexity versus the number of users for the ML MUD, the ACO based MUD and the MF aided MFAA assisted MC DS-CDMA UL at SNR = 10dB, when $N_c = 31$ -chip Gold sequences are employed.

DS-CDMA system using $N_r = 1$, $L = 1$ in conjunction with a large number of subcarriers, such as $V = 128$. However, Figs. 5 and 6 show that the BER of the ACO based MUD in the former system improved more substantially than that in the latter system, which may be explained as follows.

First of all, the BER performance of the ACO based MUD is determined by the SNR gain, which is constituted by the sum of the diversity gain and the array gain. On one hand, in the SISO MC DS-CDMA system associated with $N_r = 1$ and $L = 1$, the increased number of subcarriers V only provides a diversity gain, but no array gain. However, as shown in Fig. 6, no significant incremental diversity gain is observed by increasing the diversity order beyond $\gamma_d = 5$, which would be equivalent to $V = 5$ in a SISO MC DS-CDMA system, since the achievable diversity gain saturates, when the diversity order approaches infinity, leading to a near-Gaussian performance. By contrast, in the MFAA-assisted MC DS-CDMA system, apart from the diversity gain contributed by increasing either V or N_r , an additional array gain is achieved upon increasing either N_r or L . Furthermore, in contrast to the diversity gain, the attainable array gain does not have a strict physical upper bound, as observed in Fig. 6. Naturally, however, increasing V , N_r and L will commensurately increase the complexity imposed.

Therefore, at a given complexity, the BER performance of the ACO based MUD can be improved more substantially in the context of the MFAA-assisted MC DS-CDMA system than in its SISO counterpart, since the SNR gain achieved by employing an $L \times N_r$ MFAA in a V -subcarrier system is significantly higher than that attained by increasing the number of subcarriers V by a factor of $(N_r \times L)$ in the context of the SISO MC DS-CDMA benchmark system.

V. CONCLUSION

A sophisticated ACO-based MUD was designed for the MFAA assisted MC DS-CDMA UL, which is capable of

approaching the optimum ML performance at a significantly reduced complexity, regardless of the number of subcarriers, of the number of elements per antenna array or of the number of antenna arrays. Our simulation results also demonstrate that increasing the number of receive antenna arrays and the number of elements per antenna array in the MFAA aided MC DS-CDMA system will allow the ACO based MUD to achieve a higher BER performance improvement than that attained by increasing the number of subcarriers in the SISO MC DS-CDMA benchmark system.

REFERENCES

- [1] N. Yee, J.-P. Linnartz, and G. Fettweis, "Multi-carrier CDMA for indoor wireless radio networks," in *Proceedings of the IEEE International Symposium on Personal, Indoor and Mobile Radio Communications*, 1993, pp. 109–113.
- [2] L. Vandendorpe, "Multitone spread spectrum multiple access communications system in a multipath Rician fading channel," *IEEE Transactions on Vehicular Technology*, vol. 44, pp. 327–337, May 1995.
- [3] E. A. Sourour and M. Nakagawa, "Performance of orthogonal multi-carrier CDMA in a multipath fading channel," *IEEE Transactions on Communications*, vol. 44, pp. 356–367, Mar. 1996.
- [4] L. Hanzo, L.-L. Yang, E.-L. Kuan, and K. Yen, *Single- and Multi-Carrier DS-CDMA Multi-User Detection, Space-Time Spreading, Synchronisation and Standards*. Chichester, U.K.: Wiley, 2003.
- [5] L. Hanzo, M. Munster, B.-J. Choi, and T. Keller, *OFDM and MC-CDMA for Broadband Multi-User Communications, WLANs and Broadcasting*. Chichester, U.K.: Wiley, 2003.
- [6] L. L. Yang and L. Hanzo, "Multicarrier DS-CDMA: A multiple-access scheme for ubiquitous broadband wireless communications," *IEEE Communications Magazine*, vol. 41, pp. 116–124, Oct. 2003.
- [7] L.-L. Yang and L. Hanzo, "Performance of generalized multicarrier DS-CDMA over Nakagami- m fading channels," *IEEE Transactions on Communications*, vol. 50, pp. 956–966, June 2002.
- [8] L.-L. Yang and L. Hanzo, "Performance of generalized multicarrier DS-CDMA using various chip waveforms," *IEEE Transactions on Communications*, vol. 51, pp. 748–752, May 2003.
- [9] J. Bloch and L. Hanzo, *Third-generation systems and intelligent wireless networking: smart antennas and adaptive modulation*. Chichester, U.K.: Wiley, 2002.
- [10] M. Dell'Anna and A. H. Aghvami, "Performance of optimum and suboptimum combining at the antenna array of a W-CDMA system," *IEEE Journal on Selected Areas in Communications*, vol. 17, pp. 1030–1039, Dec. 1999.
- [11] B. Hu, L.-L. Yang, and L. Hanzo, "Performance of the smart antenna aided multicarrier DS-CDMA uplink," in *Proceedings of IEEE Vehicular Technology Conference*, vol. 1, 2004, pp. 191–195.
- [12] B. Hu, L.-L. Yang, and L. Hanzo, "Performance of the smart antenna aided generalized multicarrier DS-CDMA downlink using both time-domain spreading and steered space-time spreading," in *Proceedings of IEEE Vehicular Technology Conference*, vol. 1, 2005, pp. 458–462.
- [13] C. Xu, B. Hu, L.-L. Yang and L. Hanzo, "Performance of multi-antenna array assisted MC DS-CDMA using downlink preprocessing based on singular value decomposition," in *Proceedings of IEEE Vehicular Technology Conference*, 2007, pp. 1936–1940.
- [14] S. Verdú, *Multisuser Detection*. New York: Cambridge Univ. Press, 1998.
- [15] T. C. Fogarty, "Using the genetic algorithm to adapt intelligent systems," in *Proceedings of the IEE Colloquium on Symbols Versus Neurons*, vol. 12, 1990, pp. 4/1–4/4.
- [16] M. Jiang, S.-X. Ng, L. Hanzo, "Hybrid iterative multiuser detection for channel coded space division multiple access OFDM systems," *IEEE Transactions on Vehicular Technology*, vol. 55, pp. 115–127, Jan. 2006.
- [17] D. Fogel, "What is evolutionary computation?" *IEEE Spectrum*, vol. 37, pp. 28–32, Feb. 2000.
- [18] J. Kennedy and R. Eberhart, "Particle swarm optimization," in *Proceedings of the IEEE International Conference on Neural Networks*, vol. 4, 1995, pp.1942–1948.
- [19] M. Dorigo, L. Gambardella, M. Middendorf and T. Stutzle, "Guest editorial: special section on any colony optimization," *IEEE Transactions on Evolutionary Computation*, vol. 6, pp. 317–319, Aug. 2002.

- [20] M. Dorigo and L. Gambardella, "Ant colony system: a cooperative learning approach to the travelling salesman problem," *IEEE Transactions on Evolutionary Computation*, vol. 1, pp. 53–66, Apr. 1997.
- [21] M. Dorigo and G. Di Caro, "Ant colony optimization: a new meta-heuristic," in *Proceedings of the Congress on Evolutionary Computation*, vol. 2, 1999, pp. 1470–1477.
- [22] L. Hanzo and T. Keller, *OFDM and MC-CDMA: A Primer*. Chichester, U.K.: Wiley, 2006.
- [23] J. Boutros and E. Viterbo, "Signal space diversity: A power and bandwidth efficient diversity technique for the Rayleigh fading channel," *IEEE Transactions on Information Theory*, vol. 44, pp. 1453–1467, July 1998.
- [24] Z.-G. Yang, B. Lu and X.-D. Wang, "Bayesian Monte Carlo multiuser receiver for space-time coded multicarrier CDMA systems," *IEEE Journal on Selected Areas in Communications*, vol. 19, pp. 1625–1637, Aug. 2001.
- [25] S. L. Hijazi, A.J. Best B. Natarajan and S. Das, "Ant-colony based optimal MC-CDMA multiuser detector," in *Proceedings of the IEEE International Conference on Wireless And Mobile Computing, Networking And Communications*, vol. 1, 2005, pp. 128–132.
- [26] S. L. Hijazi, B. Natarajan and S. Das, "An ant-colony algorithm for multi-user detection in wireless communication systems," in *Proceedings of Genetic and Evolutionary Computation Conference*, 2005, pp. 2121–2126.
- [27] S. L. Hijazi and B. Natarajan, "Novel low-complexity DS-CDMA multiuser detector based on ant colony optimization," in *Proceedings of IEEE Vehicular Technology Conference*, vol. 3, 2004, pp. 1939–1943.
- [28] J.-J. Lai and J.-K. Lain, "Antenna-diversity-assisted ant-colony-based multiuser detection for DS-CDMA systems," in *Proceedings of the IEEE International Workshop on Cellular Neural Networks and Their Applications*, vol. 3, 2005, pp. 106–109.
- [29] L.-L. Yang and L. Hanzo, "Performance of generalized multicarrier DS-CDMA over Nakagami- m fading channels," *IEEE Transactions on Communications*, vol. 50, pp. 956–966, June 2002.
- [30] R. B. Ertel, P. Cardieri, K. W. Sowerby, T. S. Rappaport and J. H. Reed, "Overview of spatial channel models for antenna array communication systems," *IEEE Personal Communications Magazine*, vol. 5, pp. 10–22, Feb. 1998.
- [31] J. G. Proakis, *Digital Communications*. New York: McGraw-Hill, 2000.